



Ultrastructural Changes and Inflammatory Processes of Day-Dependent Cisplatin Administration on Rat Cardiac Tissue

Tuba Ozcan Metin¹, Gulsen Bayrak², Selma Yaman³, Adem Doganer⁴, Atila Yoldas⁵, Nadire Eser⁶,
 Duygun Altintas Aykan⁶, Banu Coskun Yilmaz⁷, Akif Hakan Kurt⁸, Mehmet Sahin⁹, Gulsah Gurbuz⁷

¹Kahramanmaraş Sutcu Imam University, Faculty of Medicine, Department of Histology and Embryology, Kahramanmaraş, Türkiye

²Uşak University, Faculty of Medicine, Department of Histology and Embryology, Uşak, Türkiye

³Kahramanmaraş Sutcu Imam University, Faculty of Medicine, Department of Biophysics, Kahramanmaraş, Türkiye

⁴Kahramanmaraş Sutcu Imam University, Faculty of Medicine, Department of Biostatistics and Medical Informatics, Kahramanmaraş, Türkiye

⁵Kahramanmaraş Sutcu Imam University, Faculty of Medicine, Department of Anatomy, Kahramanmaraş, Türkiye

⁶Kahramanmaraş Sutcu Imam University, Faculty of Medicine, Department of Pharmacology, Kahramanmaraş, Türkiye

⁷Mersin University, Faculty of Medicine, Department of Histology and Embryology, Mersin, Türkiye

⁸Bolu Abant İzzet Baysal University, Faculty of Medicine, Department of Pharmacology, Kahramanmaraş, Türkiye

⁹Gaziantep University, Faculty of Medicine, Department of Medical Biology, Gaziantep, Türkiye

Copyright@Author(s) - Available online at www.dergipark.org.tr/tr/pub/medr

Content of this journal is licensed under a Creative Commons Attribution-NonCommercial-NonDerivatives 4.0 International License.



Abstract

Aim: Cisplatin (CP) is used to treat a variety of cancers as a chemotherapeutic agent. This drug has also severe side effects and its use exhibits serious toxicity in a number of organs, including kidney and heart. The aim of the present study was to evaluate the ultrastructural and inflammatory changes induced by CP treatment in rat cardiac tissue in a time-dependent manner.

Material and Methods: Rats were randomly divided into three experimental groups; control (only saline), CP D2 (treated with CP 2.5 mg/kg/day for 2 days), and CP D7 (treated with CP 2.5 mg/kg/day for 7 days). Cardiac tissues were examined under an electron microscope. Inflammation markers including tumor necrosis factor- α (TNF- α) and interleukin 1 β (IL-1 β) were analyzed by immunohistochemistry. In addition, electrocardiography was performed to measure the electrical activity.

Results: The ultrastructural analysis of the CP D7 group revealed that myofibrils were disrupted and disorganized, mitochondria degenerated, and interstitial edema developed. When compared to the control and CP D2 groups, there was a noticeable increase in the level of TNF- α and IL-1 β expression in the CP D7 group according to immunohistochemistry results. Electrocardiography showed that RR interval was longer in CP D7 than CP D2 and control groups.

Conclusion: CP for 7 days damaged the ultrastructural morphology in cardiac tissue. Therefore, these findings suggest that the potential therapeutic approaches to reduce mitochondrial damage and inflammation against toxicity caused by CP may provide for clinically significant prevention when using the drug for an extended period of time.

Keywords: Cardiotoxicity, cisplatin, inflammation, mitochondrial damage, ultrastructure

INTRODUCTION

Cardiac damage caused by anticancer chemotherapeutic agents has become a major problem (1). Several types of anticancer drugs, including cisplatin (cis-diamminedichloroplatinum, CP) have exhibited high cardiovascular complications. CP has the ability to cure a variety of solid tumors, but its clinical application is constrained by its severe dose-dependent side effects on tissue (2).

Myocarditis, arrhythmias, congestive heart failure, cardiomyopathy, hypertension, and cardiac ischemia are among the documented cardiotoxic adverse effects of CP (2,3). The underlying mechanisms of CP-induced cardiac injury include mitochondrial dysfunction, inflammation, oxidative stress, apoptosis, and endoplasmic reticulum (ER) stress (3). Immune cell infiltration into damaged site and increased production of proinflammatory cytokines like tumor necrosis factor alpha (TNF- α), interleukin-1

CITATION

Ozcan Metin T, Bayrak G, Yaman S. Ultrastructural Changes and Inflammatory Processes of Day-Dependent Cisplatin Administration on Rat Cardiac Tissue. *Med Records*. 2023;5(3):573-7. DOI:1037990/medr.1307336

Received: 31.05.2023 Accepted: 22.07.2023 Published: 15.08.2023

Corresponding Author: Tuba Ozcan Metin, Kahramanmaraş Sutcu Imam University, Faculty of Medicine, Department of Histology and Embryology, Kahramanmaraş, Türkiye

E-mail: tubaozcanmetin@gmail.com

beta (IL-1 β), and interleukin-6 (IL-6) are indicators of inflammation, which is recognized as a key factor in cardiac tissue injury induced by the CP. Neutrophil and macrophages infiltration impair cardiac function by generating reactive oxygen species (ROS), which lead to tissue injury and cell death. Excessive ROS production causes inflammatory factors to be released, which exacerbates damage (4).

As they are the target of toxic drugs like CP, mitochondria-rich cardiomyocytes are extremely vulnerable to mitochondrial damage (5). CP accumulates in the mitochondrial matrix of cells, impairing mitochondrial respiration and producing excessive ROS (6). Thus, CP causes left ventricular dysfunction and functional abnormalities that disrupt ultrastructural morphology in mitochondria of cardiomyocytes (7). Furthermore, CP treatment has been linked to both nuclear and mitochondrial DNA damage in an experimental rat model (8). Mitochondrial targeted antioxidants may be a viable way to reduce cardiovascular problems (9).

There are very few experimental studies examining cardiovascular changes following acute CP treatment and the mechanisms underlying these changes. The goal of the current study was to evaluate the ultrastructural and inflammatory changes, and alterations in electrocardiography parameters after CP treatments in the myocardial tissue.

MATERIAL AND METHOD

Study Design

After receiving approval from Kahramanmaraş Sutcu Imam University's local ethics council for conducting animal experiments (date: 22.11.2022, protocol number 2022/11-4), the following study was conducted. Twenty-four male Wistar albino rats were housed in a controlled environment with access to food and water at a temperature of 22 \pm 3 $^{\circ}$ C and a 12-hour light and dark cycle. The Guide for the Care and Use of Laboratory Animal was followed for performing animal treatments (10). Electrocardiography (ECG) of all groups was performed under anesthesia (ketamine (75 mg/kg)-xylazine HCl (10 mg/kg) prior to CP administration for baseline values. Following electrocardiography (ECG) recordings, rats were divided randomly into 3 groups each consisted of eight rats, as listed below:

Control group (n=8): The vehicle (0.9% NaCl solution) was given intraperitoneally (ip).

CP D2 group (n=8): CP (Kocak Farma, Turkey) was injected 2.5 mg/kg/day ip for 2 days.

CP D7 group (n=8): CP was injected 2.5 mg/kg/day ip for 7 days (11).

Twenty-four hours after the last dose of the CP, ECG recordings was re-recorded. Then cardiac tissues from left ventricles of animals were rapidly removed for immunohistochemistry and electron microscopy analysis.

Electron Microscopic Examination

The ventricular tissue samples were first fixed with 2.5%

glutaraldehyde in 0.1 M phosphate buffer, followed by 1% osmium tetra-oxide post-fixation, dehydration with a graded alcohol series, cleaning with propylene oxide, and embedding in epon. Ultrathin sections were prepared for transmission electron microscopy (TEM). After that, lead citrate and uranyl acetate were used to stain the sections. The ultrathin sections were examined by TEM (JEM-1011; JEOL Ltd, Tokyo, Japan).

Immunohistochemical Analysis

The rat ventricular myocardial tissues were processed using a standard protocol, fixed in 10% formalin in phosphate buffer, and then embedded in paraffin blocks. Sections were cut at 4-5 μ m thickness on a rotary microtome (Leica 2125RT, Deer Park, IL, US) and then they were transferred to adhesive slides. The sections were incubated in Tris-EDTA solution (pH 9.0; ab93684, Abcam, Waltham, MA, USA) in the microwave to accomplish antigen retrieval. After that, the slides underwent phosphate-buffered saline (PBS) washing and 3% H₂O₂ treatment. After blocking with normal goat serum, the sections were incubated with primary antibodies for anti-TNF- α (1:100, ab6671, Abcam, Waltham, MA, USA), and anti-IL-1 β (1:100, ab9787, Abcam, Waltham, MA, USA) overnight at 4 $^{\circ}$ C. The sections were then washed with PBS before being treated with anti-rabbit IgG secondary antibody (1:200, 65-6140, Thermo Scientific, Waltham, MA, USA) for 30 min at room temperature. Following a PBS wash, the slides were incubated with horseradish peroxidase (HRP; 1: 200, 43-4323, Thermo Scientific, Waltham, MA, USA) for 10 minutes. Mayer's hematoxylin was used as a counterstain for sections following treatment with diaminobenzidine (DAB; ab64238; Abcam, Waltham, MA, USA) as a chromogen. Under a Carl Zeiss Axio Imager A2 microscope, the prepared sections were examined for immunohistochemical changes and rated as strong (++++), medium (+++), weak (++) , or absent (+) in all sections.

Electrocardiography

ECG of all rats was conducted to using a BIOPAC MP36 (Biopac Systems, Inc., Camino Goleta, CA, USA). The rats were stabilized by placing them on the experimental platform while under light anesthesia. ECG electrodes were inserted lead at derivation I ; V+, V- and ground were placed on the right-left extremities of rats. In electrode (Skintact, FS-RG1/10, Innsbruck, Austria) insertion, attention was paid to ensure that the area was hairless, wiped with alcohol, and gelled the electrodes. ECG was recorded for 2 min (0.05 100 Hz, AHA). The data were confirmed by AcqKnowledge software (Biopac Systems, Inc., Camino Goleta, CA, USA) and the analysis were saved at an appropriate time frame after the study. Parameters such as the PR interval (ms); RR interval, QT interval (ms), Tp (ms), and heart rate per minute were determined from the ECG traces.

Statistical Analysis

For statistical analysis, SPSS version 22 (IBM SPSS for Windows version 22; IBM Corporation, Armonk, New

York, USA) and R.3.3.2 software were used. The data was analyzed using One Way Anova and Shapiro-Wilk test to see if the variables followed a normal distribution. The differences in the variables that were not distributed normally between the groups were assessed using the Kruskal-Wallis H test, which was followed by a post hoc comparison test performed using the Dunn's test. The acquired data was presented as the median, 25% quartile, and 75% quartile. Statistically significant difference was defined as one with $p < 0.05$.

RESULTS

Electron Microscopic Results

Electron microscopic examination of control group (Figure 1a) showed the cardiac muscle fibers with euchromatic nucleus and rows of mitochondria between the regularly arranged bundles of myofibrils. With swollen mitochondria in between, some myofibrils in the CP D2 group (Figure 1b) appeared disorganized or disrupted. Regular arrangement of the myofibrils was almost preserved. But in contrast to the CP D2 group, the CP D7 group showed disruption and disarrangement in myofibrils, interstitial edema, dilated vacuoles in sarcoplasm, mitochondrial degeneration, and intracapillary neutrophils (Figure 1c and 1d).

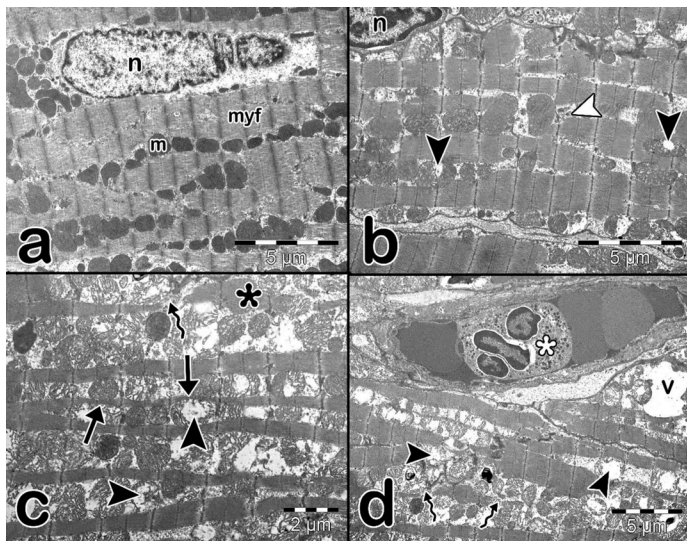


Figure 1. Electron micrographs of the myocardial muscle fibers. a (7.500×) Control group; euchromatic oval nucleus (n), rows of mitochondrion (m) and regularly arranged myofibrils (myf). b (7.500×) CP D2 group; disrupted myofibrils (white arrowhead) and swollen mitochondria (black arrowheads). c (10.000×) and d (5.000×) CP D7 group; disarrangement (asterisk), interruption (curved arrow) and local thinning (arrows) in myofibrils, dilated vacuole (v), mitochondrial degeneration (black arrowheads), and intracapillary neutrophil (white asterisk)

Immunohistochemical Results for TNF- α and IL-1 β

The immunohistochemistry staining analysis revealed that the control group's muscle fibers had weak expressions of TNF- α (Figure 2a) and IL-1 β (Figure 3a). When compared to the control group, the CP D2 group (Figure 2b and 3b) showed significantly higher immunoreactivity for both antibodies ($p < 0.001$; Figure 2d and 3d). In contrast to the findings in the control and CP D2 groups, the CP D7 group displayed a strong immunoreaction for the expression of TNF- α (Figure 2c) and IL-1 β (Figure 3c).

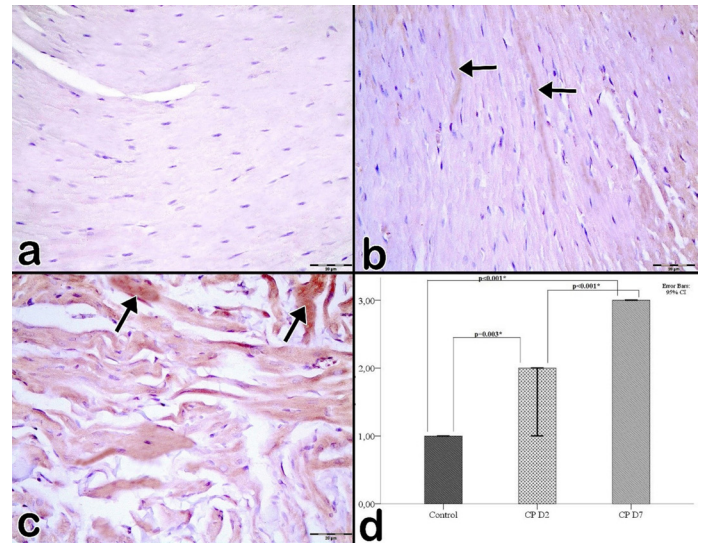


Figure 2. Representative immunohistochemical images of TNF- α in myocardium (400×). (a) Control group, (b) CP D2 group shows mild TNF- α immunoreactivity (arrows). (c) CP D7 group shows intense TNF- α immunoreactivity (arrows) in cardiac fibers. (d) Comparison of TNF- α immunoreactivity between the studied groups. Kruskal Wallis H test; statistical significance level (a): 0.05; Post-hoc: Dunn test; *The difference between groups was statistically significant. Bar statistics: Median; Error Bars: 95% confidence interval

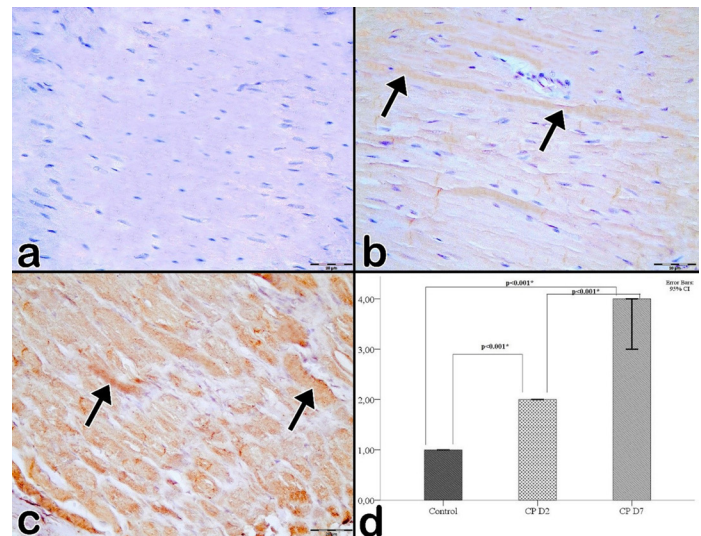


Figure 3. Representative immunohistochemical images of IL-1 β in myocardium (400×). (a) Control group, (b) CP D2 group shows mild IL-1 β immunoreactivity (arrows). (c) CP D7 group shows intense IL-1 β immunoreactivity (arrows) in cardiac fibers. (d) Comparison of IL-1 β immunoreactivity between the studied groups. Comparison of IL-1 β immunoreactivity between the studied groups. Kruskal Wallis H test; statistical significance level (a): 0.05; Post-hoc: Dunn test; *The difference between groups was statistically significant. Bar statistics: Median; Error Bars: 95% confidence interval

Electrocardiography Parameters

As shown in Table 1, comparing the CP D7 group to the CP D2 and control groups, the RR interval was longer ($p = 0.045$, $p = 0.032$, respectively). When comparing the CP D2 group to the control group, it was non-significant ($p = 0.678$). There were no differences between the groups for other ECG parameters such as heart beats per min, PR, QT, and Tp intervals.

Table 1. CP-induced ECG alterations

	Control	CP D2	CP D7	P value	Post-Hoc		
					Control-CP D2	Control-CP D7	CP D2-CP D7
QT ^a (ms), Mean±SD	0.0783±0.0153	0.0954±0.0555	0.1130±0.0544	0.618			
RR ^b (ms), Median (Q1-Q3)	0.0340(0.0270-0.3100)	0.1310(0.0320-0.1950)	0.3575(0.3190-0.4020)	0.045*	0.678	0.032*	0.045*
HB ^a (per min), Mean±SD	191.4833±21.8490	203.9800±60.0153	163.7333±36.4509	0.350			
PR ^b (ms), Median (Q1-Q3)	0.0430(0.0090-0.0590)	0.0600(0.0570-0.0620)	0.0655(0.0600-0.0840)	0.068			
Tp ^b (ms), Median (Q1-Q3)	0.0034(0.0024-0.0250)	0.0200(0.0180-0.0250)	0.0315(0.0230-0.0400)	0.098			

HB heart beats. ^aOne Way Anova; ^bKruskal Wallis H test; Post-hoc: Dunn test; alpha statistical significance level (α): 0.05; *The difference between the groups was significant

DISCUSSION

Alkylating chemotherapeutic agents like CP, have always been one of the potent drugs in overcoming human cancers (12). However, most platinum-based anticancer drugs cause cytotoxicity in tissues, which limits their clinical application (13). CP toxicity risk in a dose-dependent manner may require adjustments or stopping administration of the therapy (2). CP administration is thought to result in cardiotoxicity due to a number of mechanisms, including ER stress, mitochondrial dysfunction, oxidative stress, inflammation, and mitochondrial dysfunction (4,14,15).

Several studies have reported that CP treatment give rise to disorganization and interruption of myofibrils, mitochondrial swelling, increased area of cristae and matrix volume, ER dilation and membranous debris in a mice and rats (7,11). Similarly, our results pointed out that CP D7 group exhibited severe ultrastructural damage including loss of cristae and swelling in the mitochondria, interruption and disarrangement of myofibrils, interstitial edema, and vacuoles. CP D2 group, on the other hand, displayed mild degeneration, including disarray or disruption, with swollen mitochondria in-between some myofibrils. In some studies on mitochondrial damage caused by CP treatment, it was observed that its accumulation depletes ATP levels in cardiomyocytes, causing cell damage and cell death (16,17). Furthermore, ROS production induced by CP leads to mitochondrial functional impairment, membrane depolarization, mitochondrial swelling, and the release of pro-apoptotic factors into cytosol, which activates caspase-dependent apoptosis (2,17,18). The destruction of cellular components or increased ROS generation which cause oxidative damage, could be a consequence of damage we examined by TEM in cardiac tissue.

TNF- α and IL-1 β are two important proinflammatory cytokines that are actively involved in the inflammatory response, as is well documented. TNF- α and IL-1 β production in cardiac tissue is increased as a result of CP treatment, activating nuclear factor kappa B (NF- κ B) transcription factor. Increased TNF- α production by

cardiomyocytes recruits inflammatory cells that cause damage to surrounding cardiac tissue one week after CP injection in mice (4). It has been demonstrated that in C57BL/6 mice, inflammatory cell infiltration increased 72 hours after a single dose of CP administration (20 mg/kg, ip) (19). It is known that CP-induced oxidative stress activates inflammation (20-22). We found that the expression of TNF- α and IL-1 β was statistically higher in the CP D7 group than in the control and CP D2 groups based on the immunohistochemical results. In addition, 2 days of CP therapy increased the expression of these proteins significantly more than the control group. By increasing the expression of two important pro-inflammatory cytokines, CP administration promoted the inflammatory reactions particularly in the CP D7 group, and brought ultrastructural damage to myocardial cells, which supports our electron microscopic findings. Furthermore, some investigations have demonstrated that CP induces the production of TNF- α and IL-1 β , as well as myocardial myeloperoxidase activity in experimental studies (4,18).

The clinical data showed that supraventricular tachycardia, bradycardia and conduction abnormalities led by CP (23,24). Based on our results, CP administration prolonged the RR duration. The difference in PR, QT, Tp intervals and heart beats between the CP D2, CP D7 and control groups were not statistically significant.

CONCLUSION

CP for 7 days damaged the ultrastructural morphology in cardiac tissue. Therefore, these findings suggest that therapeutic approaches that reduce mitochondrial damage and inflammation caused by CP may provide the clinically significant prevention when using the drug for an extended period.

Financial disclosures: The authors declared that this study has received no financial support.

Conflict of Interest: The authors have no conflicts of interest to declare.

Ethical approval: Kahramanmaras Sutcu Imam University Local Animal Ethics Committee approved this study (approval number: 2022/11-4).

REFERENCES

1. Kim CW, Choi KC. Effects of anticancer drugs on the cardiac mitochondrial toxicity and their underlying mechanisms for novel cardiac protective strategies. *Life Sci.* 2021;277:119607.
2. Qi L, Luo Q, Zhang Y, et al. Advances in toxicological research of the anticancer drug cisplatin. *Chem Res Toxicol.* 2019;32:1469-86.
3. Dugbartey GJ, Peppone LJ, de Graaf IA. An integrative view of cisplatin-induced renal and cardiac toxicities: molecular mechanisms, current treatment challenges and potential protective measures. *Toxicology.* 2016;371:58-66.
4. Chowdhury S, Sinha K, Banerjee S, et al. Taurine protects cisplatin induced cardiotoxicity by modulating inflammatory and endoplasmic reticulum stress responses. *Biofactors.* 2016;42:647-64.
5. Costa VM, Carvalho F, Duarte JA, et al. The heart as a target for xenobiotic toxicity: the cardiac susceptibility to oxidative stress. *Chem Res Toxicol.* 2013;26:1285-311.
6. Demkow U, Stelmazczyk-Emmel A. Cardiotoxicity of cisplatin-based chemotherapy in advanced non-small cell lung cancer patients. *Respir Physiol Neurobiol.* 2013;187:64-7.
7. Ma H, Jones KR, Guo R, et al. Cisplatin compromises myocardial contractile function and mitochondrial ultrastructure: role of endoplasmic reticulum stress. *Clin Exp Pharmacol Physiol.* 2010;37:460-5.
8. El-Awady el-SE, Moustafa YM, Abo-Elmatty DM, et al. Cisplatin-induced cardiotoxicity: mechanisms and cardioprotective strategies. *Eur J Pharmacol.* 2011;650:335-41.
9. Bayrak S, Aktaş S, Altun Z, et al. Antioxidant effect of acetyl-L-carnitine against cisplatin-induced cardiotoxicity. *J Int Med Res.* 2020;48:300060520951393.
10. Clark JD, Gebhart GF, Gonder JC, et al. Special report: the 1996 guide for the care and use of laboratory animals. *ILAR J.* 1997;38:41-8.
11. El-Hawwary AA, Omar NM. The influence of ginger administration on cisplatin-induced cardiotoxicity in rat: Light and electron microscopic study. *Acta Histochem.* 2019;121:553-62.
12. Oun R, Rowan E. Cisplatin induced arrhythmia; electrolyte imbalance or disturbance of the SA node?. *Eur J Pharmacol.* 2017;811:125-8.
13. Wang D, Lippard SJ. Cellular processing of platinum anticancer drugs. *Nat Rev Drug Discov.* 2005;4:307-20.
14. Ma W, Wei S, Zhang B, et al. Molecular mechanisms of cardiomyocyte death in drug-induced cardiotoxicity. *Front Cell Dev Biol.* 2020;8:434.
15. Sancho-Martínez SM, Prieto-García L, Prieto M, et al. Subcellular targets of cisplatin cytotoxicity: an integrated view. *Pharmacologic Ther.* 2012;136:35-55.
16. Choi YM, Kim HK, Shim W, et al. Mechanism of cisplatin-induced cytotoxicity is correlated to impaired metabolism due to mitochondrial ROS generation. *PLoS One.* 2015;10:e0135083.
17. Varga ZV, Ferdinandy P, Liaudet L, Pacher P. Drug-induced mitochondrial dysfunction and cardiotoxicity. *Am J Physiol Heart Circ Physiol.* 2015;309:H1453-67.
18. Qian P, Yan LJ, Li YQ, et al. Cyanidin ameliorates cisplatin-induced cardiotoxicity via inhibition of ROS-mediated apoptosis. *Exp Ther Med.* 2018;15:1959-65.
19. Ueki M, Ueno M, Morishita J, Maekawa N. Curcumin ameliorates cisplatin-induced nephrotoxicity by inhibiting renal inflammation in mice. *J Biosci Bioeng.* 2013;115:547-51.
20. Xing JJ, Hou JG, Liu Y, et al. Supplementation of saponins from leaves of *Panax quinquefolius* mitigates cisplatin-evoked cardiotoxicity via inhibiting oxidative stress-associated inflammation and apoptosis in Mice. *Antioxidants (Basel).* 2019;8:347.
21. Zhou YD, Hou JG, Yang G, et al. Icaritin ameliorates cisplatin-induced cytotoxicity in human embryonic kidney 293 cells by suppressing ROS-mediated PI3K/Akt pathway. *Biomed Pharmacother.* 2019;109:2309-17.
22. El-Sawalhi MM, Ahmed LA. Exploring the protective role of apocynin, a specific NADPH oxidase inhibitor, in cisplatin-induced cardiotoxicity in rats. *Chem Biol Interact.* 2014;207:58-66.
23. Bin Naeem S, Azhar M, Baloch NU, et al. Cisplatin-induced bradycardia: a silent risk observed in two different clinical cases. *Cureus.* 2021;13:e19769.
24. H S Darling. Cisplatin induced bradycardia. *Int J Cardiol.* 2015;182:304-6.